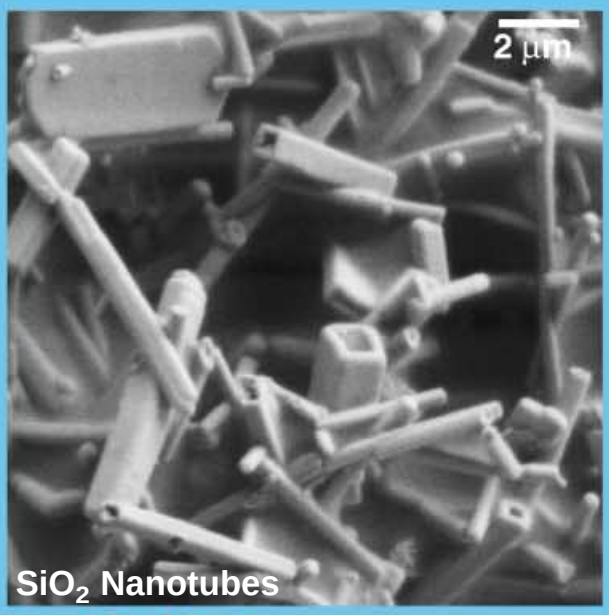

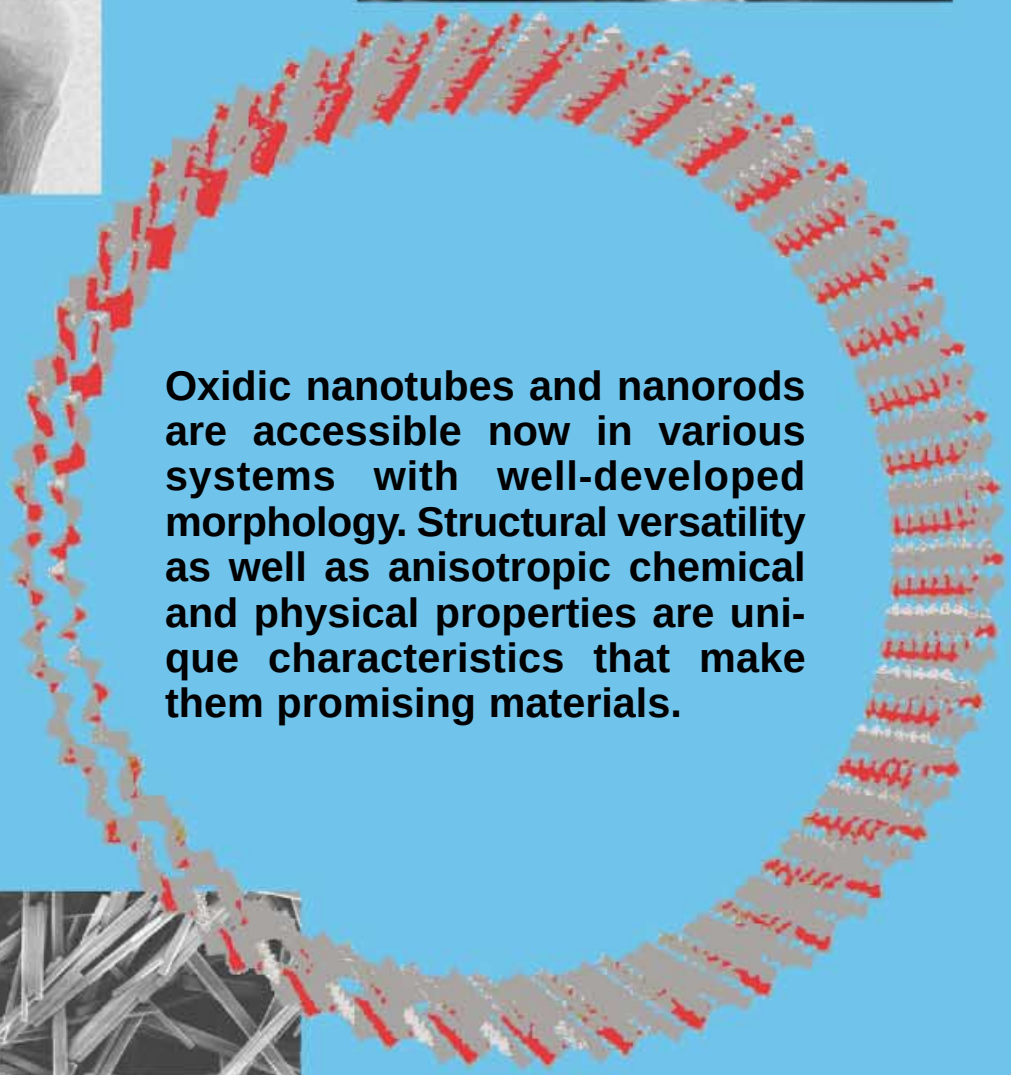

Oxidic nanotubes and nanorods are accessible now in various systems with well-developed morphology. Structural versatility as well as anisotropic chemical and physical properties are unique characteristics that make them promising materials.

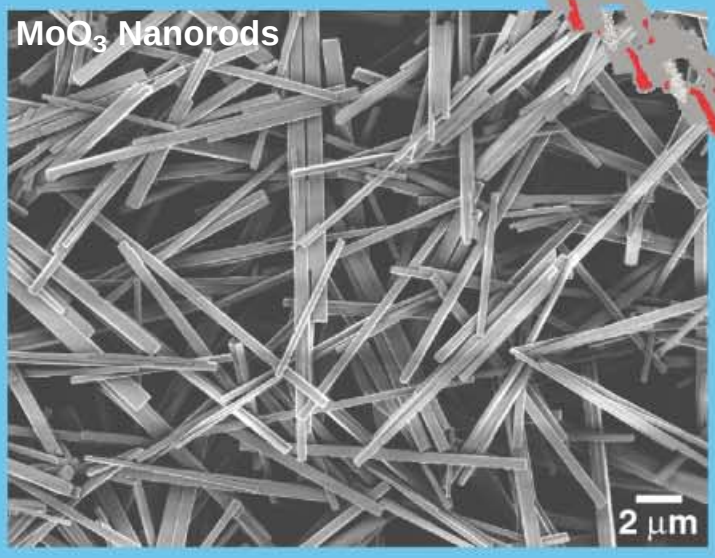

ANGEWANDTE CHEMIE

Oxidic Nanotubes and Nanorods—Anisotropic Modules for a Future Nanotechnology

Greta R. Patzke, Frank Krumeich, and Reinhard Nesper*

The discovery of carbon nanotubes in 1991 is a milestone in nanomaterials research. Since then, more and more anisotropic nanoparticles have been detected and characterized. The development of nanodevices might benefit from the distinct morphology and high aspect ratio of nanorods and nanotubes as these can be functionalized in unique ways such as incorporation of nanorods in nanotubes. Downscaling a broad range of materials to 1D nanoscopic structures is currently the focus of a rapidly growing scientific community. Developing general pathways to this goal would transfer a wide variety of properties to the nanoscale—a spectrum of phenomena so diverse that it would cover not only inorganic systems but all of materials science. Synthesis of real functional materials, however, always involves considerable synthetic ingenuity, interdisciplinary collaboration, as well as technological and economical realism. The major topic of this review is to provide a survey of recent progress in the synthesis of oxidic nanotubes and nanorods—with their non-oxidic counterparts briefly highlighted—and to outline the major synthetic routes leading to them. With the challenges of synthesizing bulk oxidic materials in mind, the establishment of trustworthy and uncomplicated ways of providing them as anisotropic nano-modules on an industrial scale appears to be more or less serendipity. Of the methods utilized in nanotube and nanorod synthesis solvothermal processes have emerged as powerful tools for generalizing and systematizing controlled syntheses of nano-morphologies. The flexibility and reliability of this synthetic approach is demonstrated here for the transformation of transition-metal oxides into high-quality anisotropic nanomaterials.

Keywords: nanorods · nanotubes · nanomaterials · oxides · solvothermal synthesis ·

1. Introduction

Entering the world of nanomaterials has become an exciting challenge for chemists, physicists, and materials scientists. During the final decade of the last century, a vast knowledge about the synthesis and properties of various nanoparticles and nanocomposites was collected, with new insights and discoveries emerging almost on a daily basis.

Now expectations concerning the application of nanomaterials as the upcoming functional materials for the 21st Century are rising: the technological limits of today's microdevices are already becoming apparent. Thus, downscaling conventional technologies by at least an order of magnitude would be the next logical step, and nanoparticles are the perfect building blocks for this purpose. This revolutionary development offers completely new dimensions when it comes to the production of nanodevices: a drastic reduction in the necessary amount of functional materials—and therefore also of price and toxicity—could turn production processes which are considered laborious and environmentally harmful into elegant "white technologies". The dimensions of nanoparticles, located between those of molecules and conventional microelectronics, allow mimicking of nature's efficient ways of managing with less when it comes to chemical and physical processing.

Moreover, physical and chemical properties of substances can be considerably altered when they are exhibited on a nanoscopic scale, and this phenomenon opens up a completely new perspective for materials design that benefits from the introduction of particle size as a new, powerful parameter.[1]

So what can stop us from getting rid of our old-fashioned techniques and shrinking them down to the economically and practically preferable nanoscale?

First of all, the multitude of nanoparticles known and their syntheses have to be mastered. This includes the scaling up of known laboratory-scale syntheses into reliable, standard manufacturing procedures for nanomaterials with uniform, monodisperse morphologies. This alone is not enough: once

[*] Prof. Dr. R. Nesper, Dr. G. R. Patzke, Dr. F. Krumeich
Laboratory of Inorganic Chemistry
ETH Hönggerberg – HCI
8093 Zürich (Switzerland)
Fax: (+41) 1-632-1149
E-mail: nesper@inorg.chem.ethz.ch

  1433-7851/02/4114-2447 $ 20.00+.50/0

readily available, these particles should then be improved by means of coating and functionalization. Moreover, there are still many substance classes remaining—especially three-and-more-element systems such as oxidic high-temperature superconductors—that have yet to be transformed into nanoscale materials. But even if all these problems have been mastered, there is another task left that must be tackled to make technological applications possible: addressing and alignment of single particles which is necessary, for example, in nanocapacitors or nanotransistors.

For alignment and functionalization procedures, nanoparticles with an anisotropic morphology are certainly advantageous. Especially nanotubes possess several different areas of contact (borders, inner and outer surfaces, and structured tube walls) that in principle can be functionalized in several ways. Their basic hollow morphology is almost directly associated with their usage as nanoscale host materials.

The most prominent examples of nanotubes are certainly the carbon nanotubes. Detailed information about the full scale of their potential and practical applications can be found in a series of review articles devoted to this topic.[2] In this regard, the up-and-coming class of oxidic nanotubes might offer even more properties and advantages leading directly to new technological applications.

But their non-hollow counterparts—nanorods and nanowires—should not be missing in a future "nano-toolbox" filled with functional nanoparticles that can be combined to design new devices. Nanorods and nanowires need not be stabilized by any kind of incorporated templating material, and the synthetic requirements for their production are surprisingly flexible. Oxidic nanorods are currently a major topic in nanoscopic research activities, and the chase for binary oxidic nanorods has been successful all over the periodic table.

Ordered arrays of both nanotubes and nanorods are accessible in principle. The combination of nanotubes and nanorods by the *tube-in-tube* or the *rod-in-tube* approach would be an outstandingly elegant means of intrinsic functionalization taking advantage both of the inner surface of nanotubes and the high aspect ratio of nanorods.

The ongoing success on all frontiers of nanomaterials research makes it more and more difficult to keep up to date with all new achievements and to derive general trends that could be the main pathways to future technology. So this article is intended to give a concise and useful survey of recent progress in synthesis and characterization of oxidic nanotubes and nanorods in combination with highlights from other materials classes. Even a short scan of novel publications concerning these topics clearly reveals that solvothermal synthesis is one of the most powerful tools providing access to distinct morphologies of nanomaterials. Selected recent examples from our laboratory illustrate the straightforward applicability of this strategy upon the production of both nanotubes and nanorods that are uniformly and quantitatively produced either in the presence of a template or via a self-organization process in solution. Sometimes it is uncomplicated "chimie douce" (soft chemistry) that provides the best results—with remarkable reliability, selectivity, and efficiency that can rarely be achieved with conventional methods.

Greta R. Patzke, born in Bremen, Germany, in 1974, studied chemistry in Hannover. She received her PhD for work on chemical transport reactions under the supervision of Professor M. Binnewies in 1999, and then she moved to the ETH Zürich to carry out work towards her habilitation. Her research interests are focused on the synthesis of nanomaterials, their structural characterization, and the application of their novel properties.


G. R. Patzke


F. Krumeich


R. Nesper

Frank Krumeich, born in Bad Hersfeld (Germany) in 1960, studied chemistry at the Justus-Liebig-Universität in Giessen and finished his doctorate 1990 with Professor R. Gruehn. After five years at the Universität Bonn and one year at the Institut für Angewandte Chemie in Berlin-Adlershof, he came to the ETH Zürich in 1997. He specializes in structural characterization by TEM methods. Besides nanomaterials, his research interests comprise bronze-type Nb-W oxides and quasicrystals (dodecagonal tantalum tellurides).

Reinhard Nesper, born in Elze/Hannover (Germany) in 1949, studied chemistry at the Universität Münster and then moved to the Max-Planck-Institut für Festkörperforschung in Stuttgart where he received his PhD under the supervision of Professor H.-G. von Schnering. Apart from a period of research with Professor Roald Hoffmann at Cornell University in 1984, he was a member of the scientific staff at the Max-Planck-Institut Stuttgart from 1978 to 1990. In 1989, he received his habilitation at the Universität Stuttgart and in 1990 he accepted the chair of inorganic chemistry at the ETH Zürich. His main areas of interest are solid-state chemistry, structure determination, and the electronic structure of solids as well as new materials, nanostructures, structure–property relationships, and models for structure formation.

2. Nanotubes

The discovery of the carbon nanotubes (CNT) by Iijima in 1991[3] in conjunction with the outstanding physical and chemical properties of this novel material has put the scientific community into a kind of continuous gold-rush mood. Up to now, immense efforts have been undertaken worldwide to optimize the synthesis, to characterize the structure, and to determine the properties of the CNTs. In addition to multi-walled CNTs, it was also possible to produce single-walled CNTs, consisting of only one concentric graphite-type layer, by co-vaporizing carbon and transition metals.[4] Various applications of CNTs have been investigated, for example, as gas detectors,[5] as field emitters,[6] as tips for scanning-probe microscopy,[7] as quantum wires,[8] and as electromechanical devices, just to mention a few.[9, 10] For a while, they also seemed to be very attractive as storage devices for hydrogen,[11] however, the earlier results could not be verified in later experiments and finally part of the storage capacity was traced back to metal impurities.[12] Semiconducting CNTs may be structurally altered in such a way that each tube becomes an electronic rectifying device,[13] while metallic CNTs are presumably able to transfer enormous current densities.[14] Of course, if CNTs would be available in large amounts at low costs, they would be an extremely versatile, novel, lightweight, high-stability material in many respects. Last but not least, it should be mentioned that the elastic properties of CNTs are beyond those of all industrial materials, utilized so far.[15]

As a side-branch of this ongoing research in the field of CNTs, structurally related nanotubes of boron nitride (BN)[16] and boron carbide (BC)[17] have been found and microscopically characterized. Furthermore, an intensive search for tubular variants of other phases has been started.[18] These studies led to the successful preparation of nanotubular forms of several oxides, which are the focus of this review, as well as of chalcogenides, which will be covered briefly. In other inorganic systems, the tubular morphology is quite rare: $NiCl_2$ nanotubes were observed as a unique example of a tubular halogen compound.[19] Metallic nanotubes are accessible from bismuth,[20] and, furthermore, membranes consisting of gold[21] and nickel[22] nanotubes, exhibiting interesting transport and magnetic properties can be obtained by using microporous alumina as a template. In addition, nanotubes of tellurium were prepared recently.[23]

In general, tubular phases cover a wide range of size, extending from mm-long hollow fibers down to nanotubes with a diameter of only a few nm. Consequently, electron-microscopy methods are the most indispensable tools for the characterization of structure and morphology.[24] As an example for oxides, needle-shaped niobium oxide crystals can be regarded as macroscopic tubes since there are channels along the needle axis.[25] This structure is most likely a result of defects, which arise under the non-equilibrium growth conditions during the preparation by chemical transport. Other examples are the hollow needles of $W_{18}O_{47}$[26] and ZnO.[27]

It is noteworthy that similar phenomena have also been observed in other systems, such as in minerals, for example, tochinolite $2Fe_{1-x}S \cdot 1.7[(Mg_{0.7}Al_{0.3})(OH)_2]$,[28] in rare-earth sialons,[29] in Ag_2Se,[30] as well as in misfit layer structures.[31] The size of other tubular oxides, such as those of titanium and vanadium, is about three orders of magnitude smaller than these microtubes, and these materials are therefore designated as oxide nanotubes. Although there is a wide agreement among scientists that the use of the term *nanotube* is restricted for the description of a material with a corresponding morphology, recently some misunderstanding has regrettably been caused by its use for specifying columnar structures, such as $Na_2V_3O_7$[32] or $MoS_2I_{0.33}$.[33] Certainly, this misuse should be avoided. Under these circumstances, it is noteworthy that S. Iijima, the discoverer of the CNTs, had designated them in his first papers modestly as microtubules of graphitic carbon. The term *nanotube* was not introduced into the literature until the following year.

At the present stage, it is important to discriminate between isolated and aggregated or fused nanotubes on the one hand and between cylinder-like tubes and scrolls on the other hand. There are a few distinct differences between the latter two such as topological flexibility, which is much larger for nanoscrolls, and dimensionality considerations. Whereas cylinder-like nanotubes are one-dimensional, nanoscrolls are still composed of layers which may have a considerable expansion when unscrolled. In this respect, scrolls may adopt one- and/or two-dimensional properties.

2.1. Vanadium Oxide Nanotubes

Considering the importance of vanadium oxide in catalysis, in electrochemistry, and as a functional ceramic, the fabrication of this material in nanostructured form and with anisotropic morphology appears to be a particularly attractive goal. The first successful approach to make a tubular vanadium oxide was with the use of carbon nanotubes as a template.[34] It was possible by exploitation of surface-tension effects to coat the CNTs externally with crystalline layers of a V_2O_5-like structure.

A fundamentally new type of vanadium oxide nanotubes (VO_x-NTs) was obtained by a soft-chemistry synthesis involving an amine with long alkyl chains as a molecular, structure-directing template.[35] This material which is available in gram amounts is mostly constructed in a scroll-like fashion. The tube diameters can be tuned from a few nanometers in the conventional VO_x-NTs up to several hundreds of nm in a new type discovered recently. VO_x-NTs are easily accessible in high yield by treating a vanadium(v) oxide precursor with an amine ($C_nH_{2n+1}NH_2$ with $4 \le n \le 22$) or an α,ω-diaminoalkane ($H_2N[CH_2]_nNH_2$ with $14 \le n \le 20$), followed by hydrolyzation, aging of the gel, and a hydrothermal reaction. The possibility of using V_2O_5, $VOCl_3$,[36] or HVO_3[37] as the vanadium source instead of a vanadium(v) alkoxide provides a low-cost alternative. Recently, the first VO_x-NTs that contain an aromatic amine were obtained with phenylpropylamine.[38]

The lengths of the VO_x-NTs vary in the range 0.5 – 15 μm and the outer diameters in the range 15 – 150 nm. Interestingly, tubes obtained with monoamines tend to form thin tube walls consisting of rather few layers (2 – 10), whereas diamines

predominantly lead to tubes with comparatively thick walls, consequently comprising a much larger number of layers (>10). As a rule, the VO_x-NTs have open ends (Figure 1a); closed tubes are scarcely observed. Vanadium oxide layers between which protonated template molecules are embedded build up the tube walls. As a result, the distance between the VO_x layers increases with increasing length of the amine or diamine applied, and interlayer distances between approximately 1.7 and 3.8 nm can be achieved in a controllable way.

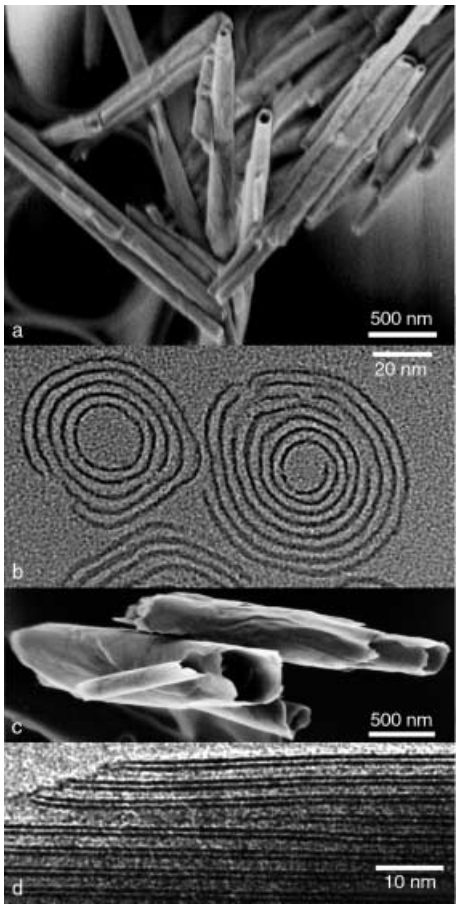

Figure 1. a) SEM image of vanadium oxide nanotubes, containing undecylamine as template (C_{11}-VO_x-NTs). The tube tips are open. b) TEM image of the cross-sectional structure of C_{16}-VO_x-NTs. The NT on the left consists of five concentric VO_x layers, that on the right of a scrolled single layer. Gaps appear at several sites in the VO_x layers. c) SEM image of vanadium oxide nanotubes obtained by addition of ammonia during the synthesis (N-VO_x-NTs). d) TEM image of the structure within the tube walls of a N-VO_x-NT. Two different interlayer distances (~0.9 nm, ~2.0 nm, template: dodecylamine) appear alternately.

Both possible types of nanotubes, namely those built up by closed concentric cylinders and those formed by scrolling one or more layers, appear in this system (Figure 1b). Most VO_x-NTs are combinations of both pure structural types and show defects, for example, gaps in the VO_x layers inside the walls.[39] The VO_x layers are crystalline as confirmed by X-ray and electron diffraction, and a 2D square lattice with a length of about 0.62 nm can describe their structure. All present experimental evidence shows that the structure of the VO_x layers is the same in all types of VO_x-NTs as well as in $BaV_7O_{16} \cdot x\,H_2O$.[40] X-ray diffraction (XRD) patterns of VO_x-NTs simulated with a structural model based on this layer structure agree well with the experimentally observed ones.[41] These layers have the composition V_7O_{16}. They consist of two sheets of VO_5 square pyramids pointing in opposite directions, and the sheets are connected by VO_4 tetrahedra (Figure 2).

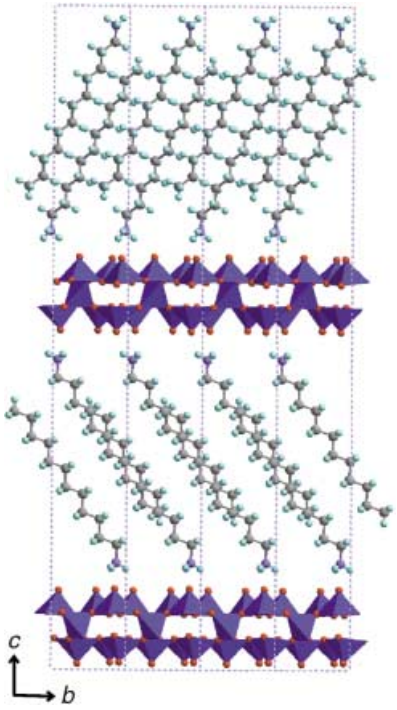

Figure 2. Structural model for the layers inside the walls of the VO_x-NTs.

Because of the scroll-type morphology, the VO_x-NTs exhibit a remarkable structural flexibility that distinguishes them from most other nanotube systems. Various exchange reactions in which the tubular morphology is well preserved are feasible. Intercalated monoamines can be substituted by diamines simply by mixing a suspension of the VO_x-NTs with the respective diamine.[42] Furthermore, a certain amount of the monoamine can be exchanged reversibly by various metal ions, for example, Na^+, K^+, Ca^{2+}, Sr^{2+}, Fe^{2+}, or Co^{2+}.[43] The possibility to insert lithium electrochemically opens up some new perspectives for battery applications; specific capacities up to 200 $mA\,h\,g^{-1}$ have been measured by several research groups.[44] However, the morphological flexibility is a drawback in this case and leads to rapid decay of the tubular morphology. Other materials turn out to be more stable under the electrochemical redox cycles.[45]

A novel type of vanadium oxide nanotube has been obtained by adding ammonia during the hydrolysis step of the synthesis.[46] These tubes have a much larger diameter, typically around 200 nm (Figure 1c). The main characteristic is the structure inside the rather thin tube wall that consists of two different, alternating, interlayer distances (Figure 1d). The larger separation is a result of the embedded amine molecules whereas it is assumed that the NH_4^+ ion is located in the narrow layers. Most likely, the structure with the shorter interlayer distance is stiffer than that with the array of amine

molecules and thus impedes bending, so causing the larger diameter of these tubes compared to the conventional VO_x-NTs. To our knowledge this type of layer structure with a regular arrangement of alternating short and long interlayer distances has been observed in a tubular phase here for the first time.

2.2. Titanium Oxide Nanotubes

Titanium oxide nanotubes (TiO_2-NTs) are accessible with varying structure and size following different routes. The first synthesis reported used a polymer mold, on which titanium oxide was deposited electrochemically.[47] The TiO_2-NT preparation in porous alumina, applying different titanium precursors, represents a similar approach.[48] The use of organic gelators generates supramolecular assemblies that form TiO_2-NTs after calcination.[49] Furthermore, polymer fibers can be used as templates: after coating with titanium oxide by a sol–gel method and removing the polymer thermally, TiO_2-NTs are obtained.[50] Another synthesis route is the anodic oxidation of titanium.[51] In these cases, the TiO_2-NTs are up to some 10 μm long and have an outer diameter of 100–200 nm while the actual wall thickness depends on the synthesis conditions applied.

TiO_2-NTs with a much smaller size have recently been synthesized by a surprisingly simple procedure. TiO_2 with anatase or rutile structure was treated with NaOH and subsequently with HCl.[52] The resulting TiO_2-NTs are 50–200 nm long and their diameter is about 10 nm (Figure 3a).

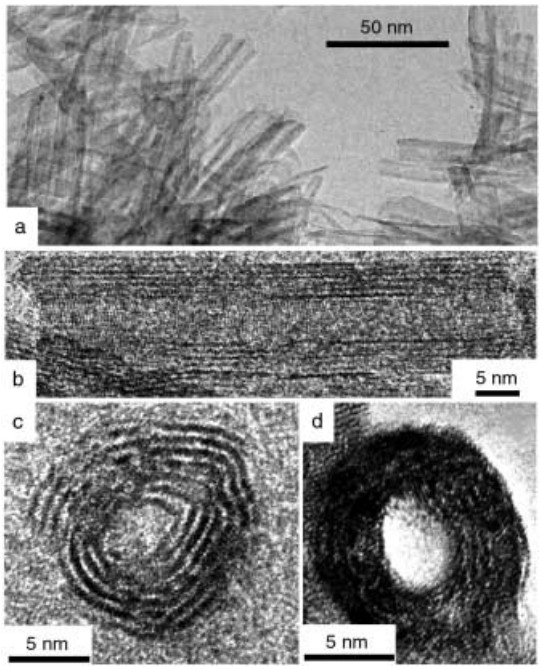

Figure 3. a) TEM image of TiO_2 nanotubes. b) HRTEM image of a well-developed, ~50 nm long NT with a diameter of ~10 nm. Lattice fringes can be seen. c) TEM image of the cross-section of a scroll-like NT. Projection along the tube axis is obtained by an embedding method for TEM preparation. d) Tube fragment that by chance is oriented parallel to the incident electron beam. This light area in the center demonstrates that the tube core is empty.

The high resolution (HR) TEM image (Figure 3b) of such a TiO_2-NT shows that the tubes have an inner core and walls. The presence of lattice fringes indicates the crystalline structure of TiO_2-NTs. Parallel fringes in the walls correspond to a distance of about 7 nm, which can also be detected as a broad reflection by X-ray and electron diffraction. The observed weak reflections indicate that the TiO_2-NTs are built in a layered titanate structure.[53, 54] The reflections of anatase, which have been detected in previous investigations,[52] are most likely caused by impurities. Views of the tube cross-section (Figure 3c) show a spiral arrangement of the dark fringes in the walls.[54] This observation requires a special TEM preparation technique that fixes the pre-orientation of the tubes by embedding them in a resin and preserves the orientation in the course of the thinning procedure.[55] The resin is apparently able to fill the tube core by capillary action, and thus the contrast of an amorphous material is observed in the tube center. On the other hand, the TEM image of a tube fragment, which is by chance oriented in the appropriate direction, shows a bright contrast in its center indicating an open channel (Figure 3d). Since the TiO_2-NTs are rather stable during thermal treatment, an application in catalysis or as a material supporting catalytic metal particles seems more probable than the use of the thermally unstable VO_x-NTs.

2.3. Other Oxidic Nanotubes

Tubular forms of silicon oxide appear in different types and sizes. It is long known that the fibrous asbestos minerals serpentine and chrysotile comprise a tubular structure that consists of curved layers.[56] For instance, the layer structure of $[Mg_3(OH)_4(Si_2O_5)]$ contains sheets of MgO_6 octahedra on one side and SiO_4 tetrahedra on the other side. This structural anisotropy causes the bending of the layers. A comprehensive TEM investigation of various chrysotile samples revealed the co-existence of fibers with spiral structures and with concentric layer structures.[57] These structural characteristics are surprisingly similar to those typical for VO_x-NTs.

In contrast to the crystalline silicate minerals, the walls of artificial tubular SiO_2 phases are generally amorphous. Silica nanotubes can be obtained by template-assisted soft chemistry routes,[58] similar to that leading to mesoporous M41-S materials,[59] or by a high-temperature approach.[60] Well-developed silica nanotubes with large diameter (up to 200 nm) and rather thin tube walls are formed by an interesting method using organic molecules as templates.[61] Derivates of cholesterol gelatinize organic solvents, and some of the resulting xerogels consist of tubular structures. The sol–gel polymerization of tetraethoxysilane occurs on the surface of these cylindrical templates, and SiO_2-NTs form after calcination. Large nanotubes of SiO_2 and TiO_2 are formed by calcination of fiberlike crystals of $[Pt(NH_3)_4](HCO_3)_2$ coated with $Si(OEt)_4$ or $Ti(OEt)_4$.[62] The tube walls consist of amorphous silicon- or titanium oxide, respectively, while the inner core is partly filled with Pt nanoparticles (Figure 4). Owing to the shape of the templat-

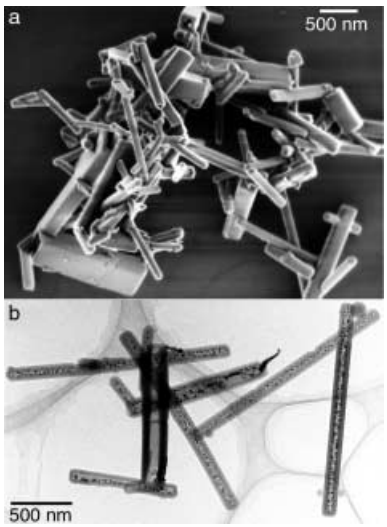

Figure 4. a) SEM image and b) TEM image of silica nanotubes filled with Pt particles, recognizable as dark spots in (b).

ing $[Pt(NH_3)_4](HCO_3)_2$ single crystals, the tube cross-sections are often rectangular.

A widely applicable route to inorganic nanotubes is to use CNTs as templates.[63] The CNTs were coated with a thin film of secondary material that builds up the tube wall after removal of the carbon. Besides vanadium oxide nanotubes (Section 2.1), this procedure generates tubular forms of SiO_2, Al_2O_3,[64] MoO_3, RuO_2,[65] and ZrO_2.[66] Of course, such secondary coatings may generally be applied to any kind of suitable primary nanoparticle to generate so-called core–shell nanosystems.

2.4. Ordering Arrays of Nanotubes

Aligned nanotubular arrays have been synthesized for different materials since the remarkable work on the MCM mesoporous phases.[67] Long known and well explored is the electrochemical route to nanotubular aluminum oxide which is prepared by anodic oxidation of Al films.[68] These porous aluminum oxide membranes can be used as a template to generate nanotube or nanorod arrays of various materials. After deposing the second material from the gas phase, by sol–gel reactions, or by other methods, the aluminum oxide is dissolved by alkaline treatment. Outstanding examples of arrays generated by this route are those of oxidic nanotubes of TiO_2,[69] In_2O_3, Ga_2O_3,[70] $BaTiO_3$, and $PbTiO_3$,[71] as well as of nanorods of ZnO, MnO_2, WO_3, Co_3O_4, and V_2O_5.[72] In this context it is interesting to note that both growth and decomposition as well as dissolution of solids may lead to the formation of arrays of aligned nanotubes or nanorods.

Quite recently, well-ordered beautiful submicrometer tubular arrays of elemental silicon have been prepared by a combination of lithographic and HF etching techniques.[73] Utilizing such arrays as chemical containers for the precipitation of secondary materials from the gas phase leads in many cases to the formation of secondary nanotubes or nanorods inside the primary tunnel systems.[74] If the primary matrix is dissolved, isolated secondary nanotubes or nanorods are created. A more comprehensive exploration of the rapidly growing research on nanoparticle arrays, however, is beyond the scope of this article.[75]

2.5. Chalcogenide Nanotubes

Microtubules of misfit layer compounds, for example, in the systems $(BiS)_{1+\delta}(NbS_2)_n$[76] and $PbNb_2S_5$,[77] have been known for a long time. Their typical diameter is in the range of a few microns, thus somewhat larger than what we would call nanotubes today. In 1992, shortly after the discovery of the CNTs, the first chalcogenide nanotubes were found for WS_2 by Tenne et al.[78] Multiwalled WS_2 nanotubes can conveniently be prepared in large amounts by treating needlelike WO_{3-x} crystals with H_2 and H_2S.[79] Alternatively, they are accessible by a chemical transport reaction[80] and by the pyrolysis of composites of WS_2 and intercalated cetyltrimethylammonium cations.[81] Similar to the CNTs, WS_2-NTs can function as tips in scanning-probe microscopy.[82]

MoS_2 nanotubes were synthesized for the first time in 1995,[83] and in the following years, a variety of synthetic routes has been developed for MoS_2 nanotubes.[84] Remarkably, a part of the tungsten content ($\sim$10 atom %) in the WS_2 nanotubes can be substituted by niobium, thereby generating novel mixed $(W,Nb)S_2$ nanotubes.[85] Most recently, NbS_2, TaS_2,[86] $MoSe_2$, and WSe_2[87] nanotubes were prepared for the first time. Here, the formation of the tubular morphology occurs during the reduction of the corresponding triselenides or selenometallates, by hydrogen. Furthermore, it is possible to coat CNTs with layers of WS_2[88] and NbS_2.[89] NbS_2 nanotubes have been modeled in advance and predicted to be stable, but the energy for bending is higher than in CNTs.[90] Similar calculations revealed that multiwalled chalcogenide nanotubes are more stable than single-walled, and, in the case of MoS_2- and WS_2-NTs these multiwalled NTs are semiconductors.[91] As the latter sulfides are excellent lubricant additives, their nanoparticular forms were tested to see if they have similar properties and gave quite promising results.[92] A further step towards an application of these materials is the possibility to store hydrogen electrochemically in MoS_2 nanotubes.[93]

A novel method for the synthesis of nanotubes of semiconducting and other chalcogenides involves organic agents. A colloid of a metastable InS phase has been obtained from tBu$_3$In and H_2S in an organic solvent in the presence of benzenethiol which acts as a catalyst.[94] As a by-product, InS nanotubes were generated. Nanotubes and nanowires of CdSe and CdS could be prepared in the presence of a surfactant.[95] In these tubes, the walls comprise nanocrystalline particles of CdSe or CdS, respectively. GaSe nanotubes have also been modeled and predicted to be stable.[96] A novel representative for nanotubes with a quite complex structure is generated by self-assembly in a colloid containing PbS nanoparticles, a polymer (poly(ethylene oxide)), and a surfactant (sodium dodecylsulfate).[97] The presence of nanotubes in this colloid was detected by means of SEM and TEM (Figure 5). Their tube walls comprise well-developed layers of PbS nanoparticles that are embedded in the organic matrix structure.

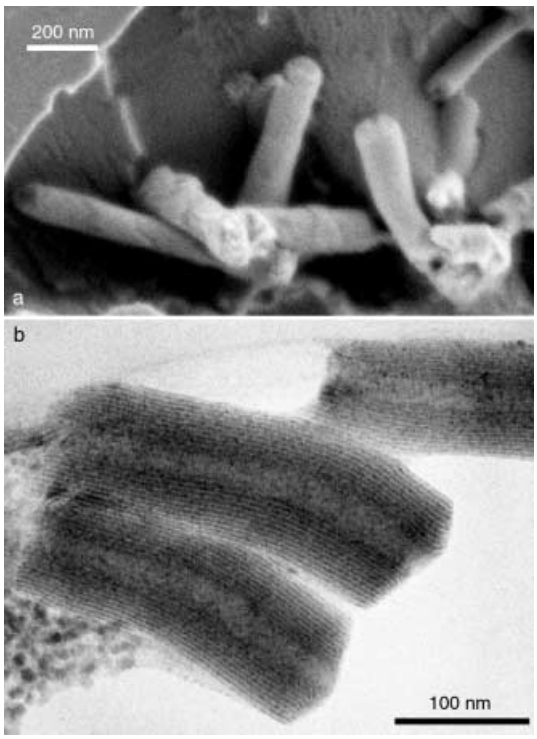

Figure 5. a) SEM image and b) TEM image of PbS nanotubes. Layers of PbS nanoparticles, which can be seen as lines with dark contrast, appear in the tube walls.

Similar to the vanadium oxide nanotubes, these PbS nanotubes also have a composite structure with an organic and an inorganic part.

2.6. Predicted Kinetically Stable Nanotubes

In addition to theoretical investigations already mentioned, there are a number of predictions that suggest quite interesting targets for the experimental chemist: a) the famous semiconductor laser material gallium nitride,[98] b) phosphorus,[99] c) silicide as well as silane forms (Figure 6a),[100] and d) GeH.[101] Also SiO_2 in form of silsesquioxane has recently been explored theoretically and found to form stable tubular nano arrangements.[102]

We have calculated possible models for V_2O_5 nanotubes as an approximation to the more complicated wall structures which have been determined for the real VO_x nanoscrolls.[35] A completely new set of potential parameters has been determined based on a series of density function calculations of binary and ternary vanadium oxides. Different coordination numbers had to be taken into account as well as a discrimination between vanadyl and bridging oxygen atoms (Figure 6b).[103]

It should be noted here, that quite frequently authors argue that general similarities to CNTs, that is, the existence of graphite-related six-ring nets, should be a prerequisite for nanotube formation. According to our experimental experience and theoretical investigations, we predict that in principle all layered materials should be convertible into tubular arrangements under suitable reaction conditions whether they form six-membered rings or are linked in other ways. If layers of a lamellar material are being separated from each other by some chemical or physical means, and if the interaction of the individual layers with their coordination shells is weak enough, there should always be the possibility of

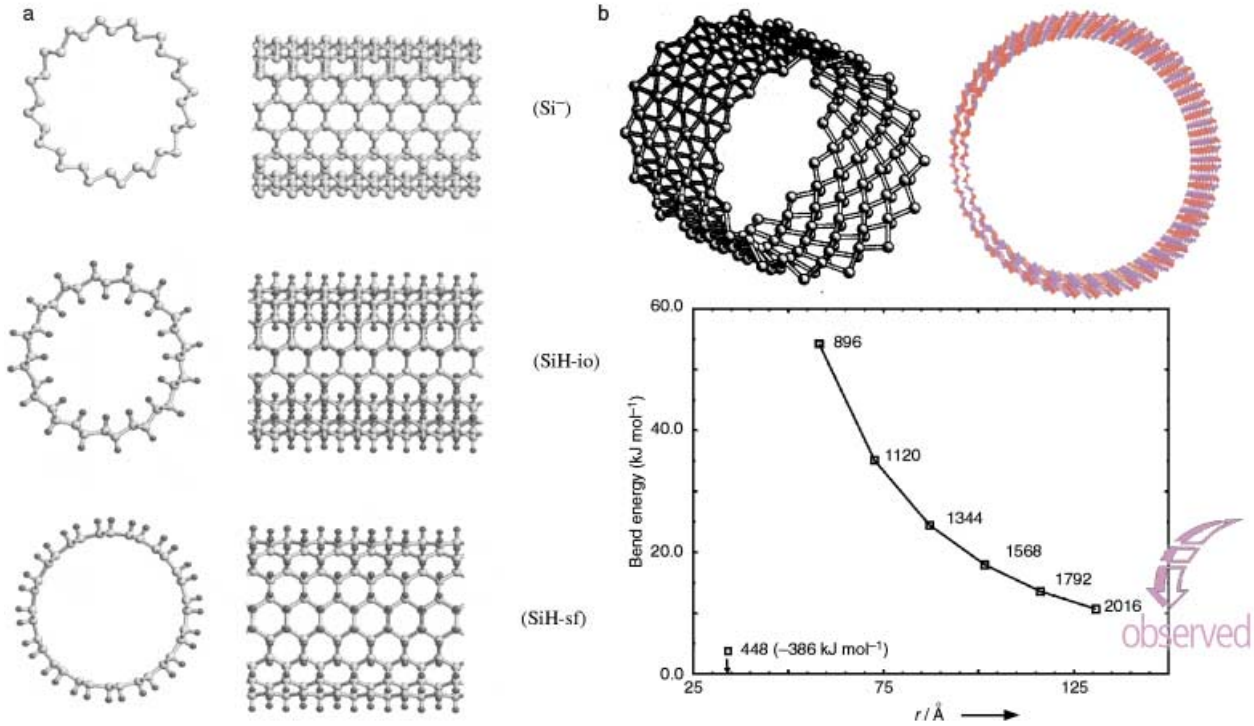

Figure 6. Predicted structures for nanotubes of a) silicides and silanes (Copyright© 2001 by APS)[100] and b) V_2O_5. Bond energies ΔE_{bend} of V_2O_5 double-layer tubes versus radius of the tubes with respect to the flat double layers (unit cell composition V_6O_{20}): $\Delta E_{bend} = E_{tube}$/ number of cells $- E_{layer}$. Both E_{tube} and E_{layer} were obtained by lattice energy minimization of the corresponding structures (ref. [103].). At each energy point, the total number of atoms in the tube is given.

self-contacts, that is, scroll formation. In the case of charged layers, this may be enhanced by local charge cancellation as a result of template coordination, for example.

3. Nanorods

Inorganic nanotubes in general are promising materials with unique properties, but they also have a common small drawback: they are rather rare—especially when it comes to complex or oxidic materials. In many synthesis processes nanorod formation frequently seems to compete with nanotube formation. Even if a reaction fulfills all prerequisites and passes through all the intermediates that are expected for the synthesis of a nanotube, the final product may still be a nanorod. Nanorods are surely morphologically less versatile host particles than nanotubes because they lack an accessible inner volume, but nevertheless, they have other advantages, such as enhanced thermal stability. So, if the sophisticated synthetic goal of producing hollow anisotropic nanostructures is sacrificed, then a wide range of synthetic routes opens up to deliver nanobelts, nanowires, and nanorods with almost any desired dimensions and aspect ratios. Redox-active materials, semiconductors, and metals can all be designed from such nanomodules which might serve in a future nanotechnology, for example, as electronic, optical, or other functional materials.

For the sake of clarity, all non-hollow anisotropic inorganic nanostructures will be addressed as "nanorods" in the following, may they have been termed rod, fiber, wire, or filament before. First, we want to discuss briefly the most important classes of inorganic nanorods, including metals, semiconductors, and carbon-containing materials, each one illustrated by a few recent, impressive synthetic examples. Then, we will turn to the topic of oxidic nanorods with emphasis on the various synthetic strategies that are employed to trigger the growth of many different oxides in 1D nanoscopic arrangements. Finally, new results concerning molybdenum oxide nanorods will illustrate the power of solvothermal synthesis, which, at present, is one of the most convenient strategies used for the design of new nanomaterials.

3.1. Inorganic Nanorods, Fibers, and Filaments

The majority of investigations dealing with inorganic nanorods is focused on the following areas: metallic nanorods, semiconductor nanorods, carbide- or nitride-based nanorods, carbon nanorods, and oxidic nanorods.

In the field of metallic nanorods, highly anisotropic nanoparticles of noble metals have attracted considerable interest as a result of their possible applications in optical, electronic, and mechanical nanodevices. Silver and selenium nanorods, for example, are generated easily and flexibly by simple reactions in aqueous solution at room temperature.

- The preparation of long, continuous silver nanowires is possible by a photochemical process employing treatment of an AgBr emulsion with a special developer containing silver nitrate. The shape of the rods is controlled by the photographic process.[104]
- Either silver nanorods or nanowires with specific aspect ratios are accessible by reduction of preformed metal-salt seeds with ascorbic acid in the presence of a surfactant. A crucial parameter here is the pH value of the reaction mixture.[105]
- Selenium nanowires are formed in the course of an unconventional bioinorganic synthesis including the reduction of selenate to selenium by the protein cytochrome c_3 as a key step.[106] There are indications that the catalytic function of this enzyme also accelerates other reduction reactions that provide nanoparticles.
- A whole series of metal and semiconductor rods of different quality has been generated inside of carbon nanotubes.[10, 107]

Once suitable sets of nanoparticles have been established they may have to be arranged in ordered arrays—a process which is essential for some applications. Recent success in the self-assembly of gold nanorods points out that soon these challenges might be mastered. Gold nanorods with an aspect ratio of 4.6:1, which have been prepared electrochemically and by precipitation methods, self-assemble into one-, two-, and three-dimensional structures. The latter can even be extended into superlattices of nanorods.[108]

Semiconductor nanorods are in the focus of current research interests.[109] In this field, the groups of Lieber and Alivisatos have contributed important synthetic strategies providing systematic approaches that can be applied to the synthesis of other materials.

- Laser-assisted catalytic growth is utilized to prepare a whole class of nanowires such as binary III-V materials (GaAs, GaP,...), ternary III-V materials (GaAs/P, InAs/P), binary II-VI compounds and binary SiGe alloys.[110] Equilibrium phase diagrams can be used to predict catalysts and growth conditions. In this way, single-crystalline nanowires with diameters as small as 3 nm can be rationally synthesized.
- A morphological series of CdSe nanocrystals including nanorods is accessible in a predictable but completely different way: Thermal decomposition of organometallic precursors in a hot mixture of trioctylphosphane oxide and hexylphosphonic acid. The various shapes are basically controlled by the ratio between the two additives which influences the relative growth rates of different faces of the emerging CdSe crystals.[111]

Carbon-based nanorods are a third major area of interest in nanorod research. It has turned out that SiC nanorods possess outstanding mechanical properties that make them promising candidates for any kind of reinforcement in the design of composite materials. Again, the variety of possible synthetic approaches and the successful mastering of the crucial alignment step can be demonstrated by two recent examples:

- The reaction of aligned carbon nanotubes with SiO at 1400 °C affords highly aligned SiC nanorods with well-separated, nanowire tips. Moreover, these arrays exhibit excellent field emission properties together with a unique combination of elasticity and strength.[112]

- β-SiC nanorods with diameters from 10 to 40 nm and lengths up to several micrometers are available even at temperatures 1000 °C lower than the above mentioned synthesis: hydrothermal reactions can also be applied for carbide-nanorod formation, and in the case of SiC the starting materials are $SiCl_4$, CCl_4, and Na.[113]

3.2. Oxidic Nanorods

Oxidic nanoparticles are essential for the design of superconductors, semiconductors, sensors, and many other devices in a future nanotechnology. Therefore, a general synthetic access is needed for their large-scale preparation. From the scientific point of view, transforming the manifold of technically relevant oxidic materials into 1D nanostructures offers fundamental opportunities for investigating the effect of size and dimensionality on their collective optical, magnetic, and electronic properties.

Oxidic nanorods in particular have raised scientific interest because of the observation of high critical current densities in nanorod-superconductor composites, such as MgO nanorods incorporated in $AgBi_2Sr_2CaCu_2O_8$.[114] The introduction of nanorods improves the performance of the superconductor dramatically and is thus an important step towards large-scale applications, because the critical current densities need to be enhanced considerably in these materials.

Table 1 contains a survey of recent research activities concerning the synthesis of oxidic nanorods. A closer look at the multitude of available materials, however, reveals the general trends and, moreover, certain challenges that remain to be tackled:

- First of all, the variety of different synthetic routes is obvious. There are many quite successful strategies employed for specific targets, but: there is no general guideline that could be consulted for the design of any kind of desired novel nanorods.
- This problem could be overcome by the concise study of the underlying mechanistic processes that lead to the formation of 1D nanoscopic structures. Up to now, only a minority of the publications in this area really deliver synthetic guidelines and explanations that can be productively applied to the synthesis of other classes of nanorods. To save the extensive optimization work that precedes many brilliant nanorod syntheses, it is necessary to devote more efforts on fundamental mechanistic studies. Such attempts will certainly be favored by joint collaborations on mechanistic investigations in catalysis, biomineralization, and nanosciences.
- Nevertheless, there are some major synthetic methods that are often successfully employed for nanorod formation: gas-phase reaction methods, solvothermal routes, template-directed as well as liquid-crystal assisted syntheses, various solution-based techniques, and sonochemically driven reactions are widely used. So when it comes to the development of new nanorod syntheses, there are at least some principal pathways that are likely to be successful. For many oxides, gas-phase thermochemical syntheses seem to prevail, however, a continuous search for low-temperature alternatives is under way.

Table 1. Synthetic routes for oxidic nanorods (published since 1995).

Oxide	Synthetic route	Ref.	Oxide	Synthetic route	Ref.
$BaCrO_4$	Fusion of reverse micelles and microemulsion droplets	[122]	MnO_2	Template method with alumina membranes	[127]
$BaSO_4$	Precipitation from aqueous solution in presence of polymers	[123]	MnO_2	Hydrothermal synthesis	[142]
$BaWO_4$	Reversed micelle templating method	[124]	MoO_3	Template-directed reaction of molybdic acid and subsequent leaching process	[143]
CdO	Evaporation of metal oxide powders at high temperatures	[125]	MoO_3	Templating against carbon nanotubes	[65]
$CdWO_4$	Hydrothermal treatment of $CdCl_2$ and Na_2WO_4	[126]	MoO_2	Templating against carbon nanotubes	[65]
Co_3O_4	Template method with alumina membranes	[127]	$PbTiO_3$	Sol-gel electrophoresis, deposition in polycarbonate membrane	[144]
CuO	Room temperature reaction of $CuCl_2 \cdot 2H_2O$ and NaOH with PEG 400	[128]	RuO_2	Templating against carbon nanotubes	[65]
Fe_2O_3	Thin-film processing method	[129]	Sb_2O_3	Microemulsion method for the system AOT–water–toluene[a]	[145]
Fe_3O_4	Sonication of aqueous iron(II) acetate in the presence of β-cyclodextrin	[130]	Sb_2O_5	Microemulsion method for the system AOT–water–toluene[a]	[145]
Ga_2O_3	DC arc discharge of GaN powders in Ar/O_2 mixture	[131]	Sb_2O_5	Templating against carbon nanotubes	[65]
Ga_2O_3	Gas reaction method starting from Ga and O_2 at 780 °C	[132]	SnO_2	Annealing of powders generated from inverse microemulsions	[146]
Ga_2O_3	Physical evaporation at 300 °C from a bulk gallium target	[133]	SnO_2	Evaporation of metal oxide powders at high temperatures	[125]
Ga_2O_3	DC arc discharge (GaN, graphite, nickel powder)	[134]	SiO_2	Helical mesostructured tubules from Vortex-Assisted Surfactant Templates	[147]
Ga_2O_3	Electric arc discharge of GaN powders mixed with Ni and Co	[135]	TiO_2	Sol-gel template method employing alumina membranes	[148]
Ga_2O_3	Heating of Ga with SiO_2 powder and a Fe_2O_3 catalyst	[136]	V_2O_5	Vanadium pentoxide gels	[149]
GeO_2	Carbon-nanotube confined reaction of metallic Ge	[137]	V_2O_5	Templating against carbon nanotubes	[65]
In_2O_3	Evaporation of metal oxide powders at high temperatures	[125]	WO_3	Templating against carbon nanotubes	[65]
In_2O_3	Growth from Au droplets	[138]	YBCO	Laser ablation of a high T_c superconductor $YBa_2Cu_3O_7$	[150]
IrO_2	Templating against carbon nanotubes	[65]	ZnO	Gas reaction employing Zn and H_2O	[151]
$K_2Ti_6O_{13}$	Calcination of KF and TiO_2	[139]	ZnO	Evaporation of metal oxide powders at high temperatures	[125]
MgO	Vapor-solid growth process with in situ generated Mg vapor	[114]	ZnO	Catalyzed epitaxial growth	[152]
MgO	Heating of $MgCl_2$ at 750 °C in mixture gas (Ar/H_2)[b]	[140]	ZnO	Self-organization of nanoparticles	[153]
$Mg(OH)_2$	Solvothermal treatment of Mg, H_2O, and ethylenediamine	[141]			

[a] AOT = sodium bis(2-ethylhexyl)sulfosuccinate. [b] The quartz apparatus is probably the oxygen source.

- In recent years, rapid progress has been made in the transformation of binary oxides into anisotropic 1D nanoscale morphologies—but the series of binary oxidic nanorods is far from complete. Even if this goal has been fulfilled, the great variety of ternary and higher oxidic nanorods still remains to be discovered—and with them possible drastic enhancements of their manifold properties which are already fascinating in the bulk materials.

Three recent publications reveal how the main synthetic strategies are employed in an elegant and effective way.[115] Solvothermal syntheses will be treated in the next section.

High-temperature evaporation of metal oxides: This surprisingly uncomplicated technique starts out from commercially available oxides of zinc, tin, indium, cadmium, and gallium which are placed at the center of an alumina tube that is subsequently inserted in a tube furnace.[125] The evaporation temperatures are determined on the basis of the melting point of the oxides. As a result, perfectly shaped nanobelts of the semiconducting oxides are deposited. They exhibit wire-like nanostructures with remarkable lengths that even extend to the millimeter scale.

Reverse micelle- and micro-emulsion templating synthesis: This technique was utilized to generate uniform oxide materials such as $BaWO_4$ nanorods.[124] The problem of particle alignment is tackled during the synthesis, because as-made assemblies consisting of arrangements in side-by-side geometry are formed. Similar nanorod superstructures of $BaWO_4$ are also produced as Langmuir–Blodgett monolayer assemblies.

Sonochemical processing of aqueous solutions: Magnetite nanorods are accessible by straightforward ultrasound irradiation of aqueous iron(II) acetate solutions in the presence of β-cyclodextrin which acts as a size-stabilizing agent. The starting material is converted quantitatively into nanorods by three hours of sonication.[130]

3.3. Solvothermal Synthesis of Molybdenum Oxide Nanorods: A Case Study

Solvothermal synthesis is one of the most powerful strategies employed in nanochemistry. Especially when exposed to supercritical conditions, many starting materials undergo quite unexpected reactions that are often accompanied by the formation of nanoscopic morphologies, which are not accessible by classical routes.

Another benefit from solvothermal synthesis is the wide variety of parameters that can be chosen and combined: reaction temperatures close to room temperature or as high as several 100 °C, variations in pH value of the systems, choice and concentration of solvents, introduction and removal of templates and other additives, choice of different autoclave geometries, etc.[116] Combinatorial methods might be a suitable approach towards systematization of these parameter fields—but the problem of subsequent scale-up procedures always remains to be solved after a breakthrough in solvothermal combinatorial synthesis.

If, however, a standard procedure for solvothermal formation of nanoparticles has been established, then these solvothermal reactions are outstandingly efficient (almost 100% conversion of the starting material), time-saving, and experimentally effortless, such as the low-cost synthesis of vanadium oxide nanotubes (see Section 2.1).[36]

3.3.1. Nanorods of α-$MoO_3 \cdot H_2O$ and MoO_3: Template-Directed versus Template-Free Solvothermal Syntheses

The solvothermal syntheses of $MoO_3 \cdot H_2O$[143] and MoO_3 nanorods[117] are especially suitable to demonstrate the differences in template-directed and template-free solvothermal approaches—and the effectiveness of these pathways.

When planning a solvothermal synthesis of nanoparticles with a distinct anisotropic morphology, it is always convenient to start from an educt with a layered structure, especially when a template is involved. Therefore, both of the nanorod syntheses discussed here have the same starting material in common: yellow molybdic acid, $MoO_3 \cdot 2H_2O$. This precursor is cheap, easy to synthesize in large amounts, and air and moisture stable. The layered structure of this host compound facilitates direct intercalation of template molecules such as neutral primary amines with long alkyl chains. Yellow molybdic acid consists of $[MoO_5(H_2O)]$ octahedra connected in infinite layers with water molecules intercalated in between.[118] There are two kinds of differently bound water molecules which can be removed in a topotactical reaction proceeding in two steps.[119] This reaction sequence, however, is observed neither during $MoO_3 \cdot H_2O$ nanorod formation nor in the template-free route leading to nanorods of MoO_3. So how do these reactions proceed?

3.3.2. Template-Directed Formation of $MoO_3 \cdot H_2O$ Nanorods

The synthesis of $MoO_3 \cdot H_2O$ nanorods is basically carried out in two steps. First, $MoO_3 \cdot 2H_2O$ undergoes an intercalation of amines and a lamellar composite material is formed. This intermediate is then treated with HNO_3, and a leaching process takes place which removes the amine from the intercalation compound. As a result, template-free $MoO_3 \cdot H_2O$ nanofibers are quantitatively formed.

The first step includes addition of amine and distilled water, followed by aging at room temperature for at least 48 hours. The subsequent hydrothermal treatment is remarkably insensitive towards changes in time. The temperature may range between 100 and 120 °C: no matter how long the duration of the hydrothermal treatment (from 1 up to 14 days), the lamellar phase is always formed. At higher reaction temperatures, more caution must be exercised when choosing the appropriate reaction time. Finally, the intercalation process is completely inhibited at 180 °C. So there is a relatively wide window of possible reaction parameters. The lamellar product for dodecylamine as an intercalate can be expressed by the general formula $(C_{12}H_{28}N)_{0.5}MoO_{3.25}$ and exhibits interlayer distances of 2.76 nm (Figure 7a). Generally, several long-chained primary amines ($C_nH_{2n+1}NH_2$ with $11 \leq n \leq 16$) can serve as templates.

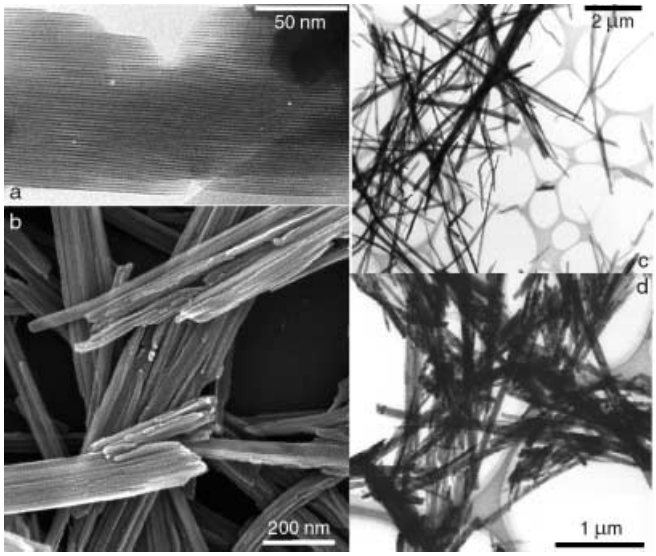

Figure 7. a) TEM image of the layered molybdenum oxide amine composite containing dodecylamine as a template. b) SEM image of several bundles of $MoO_3 \cdot H_2O$ fibers. c) Representative TEM image of $MoO_3 \cdot H_2O$ fibers consisting of smaller filaments. d) Representative TEM image of molybdenum oxide fibers after heating at 400 °C in air for several hours.

During the second step the template is leached out again to give the final product. For this purpose, stirring the mixture for 2 days at room temperature with 33 % HNO_3 is sufficient. At first glance, the formation of a mesoporous material could reasonably be expected, however, a morphological transformation is observed instead: The lamellar composite material is turned into fibers, which corresponds to the conversion of a 2D into a 1D nanoscopic material. As a result, $MoO_3 \cdot H_2O$ fibers with an approximate diameter around 140 nm and an average length of 5 μm are formed (Figure 7c), which exhibit an interesting morphological feature: SEM micrographs reveal that they indeed form bundles of agglomerated smaller filaments with diameters ranging from 20 to 50 nm (Figure 7b).

This filament-like shape in the nanoscale dimension leads to the exposure of a large fraction of the atoms to the surface. Thus, these materials are promising candidates for the development of new catalytic materials. Molybdenum oxides are indeed important and effective catalysts in alcohol[120] and methane oxidation.

Finally, the fibers withstand thermal treatment at 400 °C. Their morphology remains almost unchanged, although they are converted into MoO_3 (Figure 7d). There is, however, a much more simple and elegant route to quickly generate large amounts of MoO_3 nanorods.

3.3.3. *Template-Free Formation of MoO_3 Nanorods*

The synthetic procedure for the direct transformation of $MoO_3 \cdot 2H_2O$ into MoO_3 nanorods can be outlined quite briefly: autoclave treatment of the starting material with small amounts of a solvent, preferably an acid, results in the quantitative formation of fibrous MoO_3. The progress of the reaction can even be monitored optically, because the yellow molybdic acid is turned into the blue nanorod material. This process combines two benefits that seem to be rather contradictory at first sight: although the reaction in general is remarkably stable towards changes in parameters, the morphology of the emerging rods can still be controlled by varying the conditions! So what is going on with the yellow molybdic acid here?

In a standard procedure, $MoO_3 \cdot 2H_2O$ is simply treated with diluted glacial acetic acid in an autoclave (180 °C, 7 days). Plain nanorods with an average diameter of 100 – 150 nm and lengths on the microscale (3 – 8 μm) are formed quantitatively (Figure 8). After washing off the acid and drying in air, the product is pure.

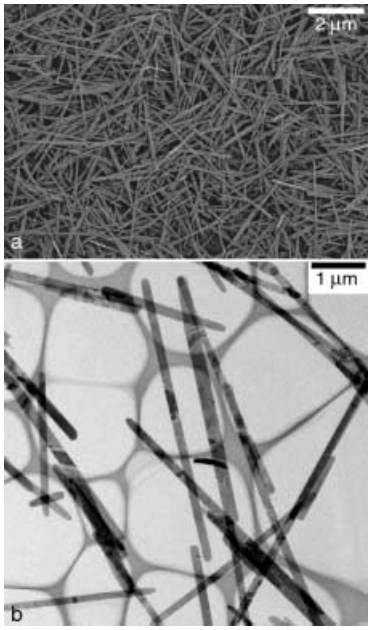

Figure 8. a) SEM and b) TEM images of MoO_3 fibers after 7 days of hydrothermal treatment in acetic acid.

The parameters time and temperature can be chosen from a wide range. Systematic investigations indicate the minimum experimental requirements necessary for the formation of nanorods: At 80 °C, practically no product formation can be observed, because most of the yellow molybdic acid is dissolved. Complete dissolution of the starting material without any product formation occurs when the temperature is raised to 180 °C with the reaction time limited to 1 day. Thus, the onset of the reaction requires temperatures around 90 °C and at least two or three days reaction time. Figure 9 shows the transition from finely shaped to thicker rods when the temperature is increased stepwise from 90 °C to 180 °C. Thus, the morphology of the rods can be directed by appropriate choice of temperatures below 180 °C.

From a mechanistic point of view, the fact that the educt is first dissolved completely and then precipitates again clearly excludes any kind of topotactic reaction. Consequently, the connection between success of solvothermal treatment and pre-structured layers in the educt is lost here, which suggests that much more anisotropic morphologies may be generated in this straightforward fashion. Therefore, a thorough investigation is under way to generalize the underlying reaction principle and so to exploit it for the synthesis of other nanomaterials.

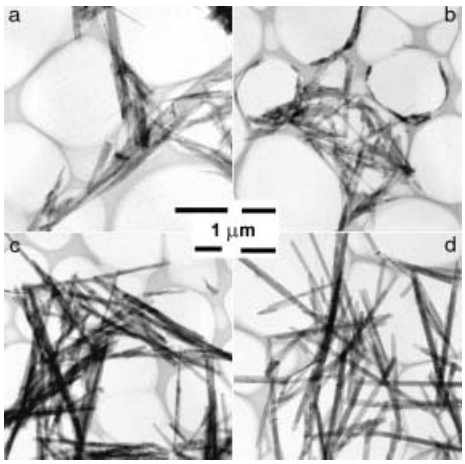

Figure 9. Representative TEM images of MoO_3 nanorods after 3 days of hydrothermal treatment in acetic acid at different temperatures: a) 90 °C, b) 120 °C, c) 150 °C, d) 180 °C.

The pH value of the reaction mixture is an even more powerful factor than the temperature when nanorods of specific diameters are to be synthesized. By appropriate choice of an acidic solvent, nanorod diameters ranging from the microscopic scale down to about 100 nm are accessible. The MoO_3 fibers can gradually be tuned by changing the diluted acid (Figure 10). This principle can be used to meet the specific needs of industrial applications and it can be further refined by combination with the influence of temperature on the morphology.

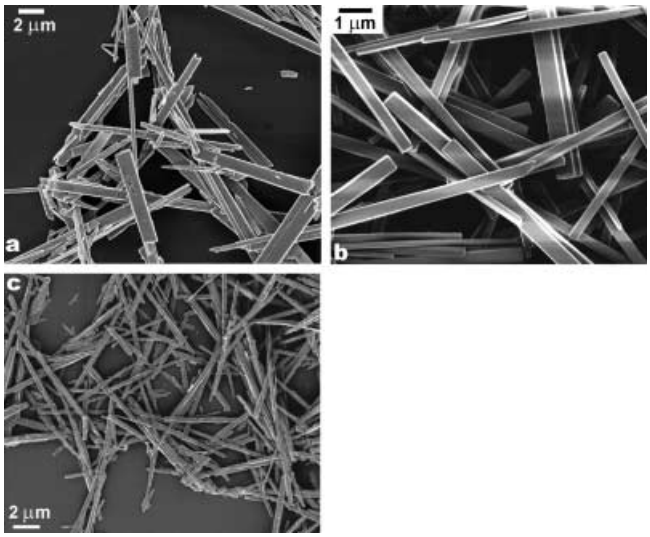

Figure 10. SEM images of MoO_3 nanorods showing the effect of acid addition: a) H_2SO_4, b) HCl, c) salicylic acid.

In summary, these $MoO_3 \cdot 2H_2O$–solvent systems are confined to a few elementary components. Therefore, they are predestined for fundamental studies elucidating the mechanisms of solvothermal processes. The products exhibit a distinct anisotropic morphology in almost 100% yield with no particle agglomerations. Therefore, morphological changes related to variation of parameters can be detected unambiguously and immediately. In principle, MoO_3 nanorods are formed in an outstandingly high yield within a very wide scope of experimental conditions with little synthetic effort. Thus, this synthetic approach is a good and stable candidate for industrial manufacturing in scaled-up processes.

3.4. General Trends in Nanotube and Nanorod Syntheses

"Trained serendipity" is surely one of the most reliable companions of chemists. The "training", of course, is a profound chemical knowledge combined with naïve curiosity and freeflying fantasy. Though we are far beyond betting on chance synthetic chemistry still requires an element of luck, and this is especially true for designing the nano regime. Quasicrystals and fullerenes could have been detected long before the eighties but have simply been in the shadow of other scientific discoveries and went unnoticed. Some general trends are emerging in the design of nanotubes and nanorods:

- Growth out of nanoscopic catalyst drops as realized for CNTs and for semiconductor nanorods
- Condensation or polymerization inside or outside of nanotubular structures
- Scrolling of layered materials either starting directly from the bulk solids or from lamellar intermediates
- Nanorod formation on ion exchange in nanotubular or lamellar materials—cation against H^+ ions—leading to a densification of morphology
- Stacking of tori (rings) in a freestanding manner or aided by nanotubes or rods
- Moulding by use of tenside template solutions or liquid-crystal structures with or without external fields
- Sonication in suitable solvents. Surprisingly, acid treatment of single-walled CNTs under supersonication can lead to formation of carbon rings and tori.[121]

The general trick of course would be a surface-directed growth process if one knew and could design selected surface coverages under synthesis conditions. This technique would go much beyond biomineralization because it is not restricted to the use of "biomolecules". Furthermore, this fundamental problem in materials design, catalysis, biomineralization, and nanoelectronics will benefit from the interdisciplinary exchange of ideas circumventing historical research borders.

4. Summary and Outlook

Despite of being mainly focused on oxidic systems, this review clearly reveals the vast amount of knowledge that has been gained in the last ten years on anisotropic nanoscopic materials and the enormous potential these materials have for nanotechnology. The discovery of the carbon nanotubes in 1991 has catalyzed a fruitful and still growing interest in nanotubes and nanorods, both in application-oriented industrial as well as in basic research. Although carbon nanotubes are still the most widely investigated examples for such materials, especially regarding potential applications, the world-wide search in other systems is steadily increasing this structural family. This growing diversity is not only because of an extension of the systems investigated but also to the skillful

application of a wide range of different synthetic methods. Prominent among them are soft chemistry routes that involve sol–gel reactions and that frequently employ organic molecules as structure-directing templates. For example, such procedures are utilized to generate nanotubes of vanadium and titanium oxide as well as molybdenum oxide fibers. This approach is outstanding because of the high yield and the high purity of the products. Another versatile method is the use of pre-structured materials. They are acting as structure-directing templates as well, but the term *template* is used here to designate a nano- or even microstructured material rather than a molecule as in the case of the above-mentioned soft chemistry routes. These templates can be anisotropic particles themselves, such as carbon nanotubes or polymer fibers, which are coated with a second material and are removed afterwards. Alternatively, the template can be a porous material, such as aluminum oxide, in which the pores are filled with a second material. After dissolution of the aluminum oxide, the nanotubes or nanorods remain. It is this inventiveness concerning new sophisticated synthetic pathways that promises to be the basis for the discovery of many more new and useful anisotropic materials.

However, it is not only the synthetic capability that has increased immensely in recent years, but also the optimization of the analytical tools and their wide availability that contribute to a better characterization of these materials. For instance, without electron microscopes with high resolution, several of the nanotubular phases might have slipped the attention of the researchers.

The interesting physical and chemical properties of strongly anisotropic materials, such as, nanotubes and nanorods quite often differ from those of the corresponding bulk material and those of isotropic nanoparticles. The usefulness of these properties for various applications is mentioned in this review. However, it must be stated that this is only the beginning. Because of ongoing attempts to further miniaturize electronic, optical, and mechanical components, there is a need for materials that could be used as building blocks in the size region of a few nanometers. Considering these perspectives, we are sure that the role of nanotubes and nanorods in a future nanotechnology can hardly be overestimated.

In a much more advanced stage of technology well-designed nanoparticles may then become the larger hosts for molecular devices—molecular in the original meaning of the term. For further optimization of presently utilized materials, nanotechnology anyhow is an imperative.

Our research was generously supported by the ETH Zurich (TEMA – Templated Materials), by the Swiss National Science Foundation (MaNEP – Materials with Novel Electronic Properties), and by the National Research Program "Supramolecular Functional Materials".

Received: December 13, 2001 [A 506]

[1] C. N. R. Rao, A. K. Cheetham, *J. Mater. Chem.* **2001**, *11*, 2887; C. N. R. Rao, G. U. Kulkarni, P. J. Thomas, P. P. Edwards, *Chem. Eur. J.* **2002**, *8*, 29.

[2] P. M. Ajayan, *Chem. Rev.* **1999**, *99*, 1787; N. Grobert, *Nachr. Chem. Tech. Lab.* **1999**, *47*, 768; P. M. Ajayan, O. Z. Zhou, *Top. Appl. Phys.* **2001**, *80*, 391.

[3] S. Iijima, *Nature* **1991**, *354*, 56.

[4] S. Iijima, *Nature* **1993**, *363*, 603; D. S. Bethune, C. H. Kiang, M. S. De Vries, G. Gorman, R. Savoy, J. Vazques, R. Beyers, *Nature* **1993**, *363*, 605.

[5] J. Kong, N. R. Franklin, C. Zhou, M. G. Chapline, S. Peng, K. Cho, H. Dai, *Science* **2000**, *287*, 622; P. G. Collins, K. Bradley, M. Ishigami, A. Zettl, *Science* **2000**, *287*, 1801.

[6] A. G. Rinzler, J. H. Hafner, P. Nokolaev, L. Lou, S. G. Kim, D. Tomanek, P. Nordlander, D. T. Colbert, R. E. Smalley, *Science* **1995**, *269*, 1550; W. A. de Heer, A. Chatelain, D. Ugarte, *Science* **1995**, *270*, 1179; Q. H. Wang, A. A. Setlur, J. M. Lauerhaas, J. Y. Dai, E. W. Seelig, R. P. H. Chang, *Appl. Phys. Lett.* **1998**, *72*, 2912.

[7] H. J. Dai, J. H. Hafner, A. G. Rinzler, D. T. Colbert, R. E. Smalley, *Nature* **1996**, *384*, 147.

[8] M. H. Devoret, H. J. Dai, A. Thess, R. E. Smalley, L. J. Gerlings, *Nature* **1997**, *386*, 474.

[9] P. Pocharal, Z. L. Wang, D. Ugarte, W. A. de Heer, *Science* **1999**, *283*, 1513.

[10] C. N. R. Rao, B. C. Satishkumar, A. Govindaraj, M. Nath, *ChemPhysChem* **2001**, *2*, 79.

[11] A. C. Dillon, K. M. Jones, T. A. Bekkedahl, C. H. Kiang, D. S. Bethune, M. J. Heben, *Nature* **1997**, *386*, 377.

[12] M. Hirscher, M. Becher, M. Haluska, U. Dettlaff-Weglikowska, A. Quintel, G. S. Duesberg, Y.-M. Choi, P. Downes, M. Hulman, S. Roth, I. Stepaneck, P. Bernier, *Appl. Phys. A* **2001**, *72*, 129; C. Zandonella, *Nature* **2001**, *410*, 734.

[13] P. Lambin, A. Fonseca, J. P. Vigneron, J. B. Nagy, A. A. Lucas, *Chem. Phys. Lett.* **1995**, *245*, 85; A. Fonseca, E. A. Perpète, P. Galet, B. Champagne, J. B. Nagy, J. M. André, P. Lambin, A. A. Lucas, *J. Phys. B* **1996**, *25*, *4915*; V. Meunier, L. Henrad, P. Lambin, *Phys. Rev. B* **1998**, *57*, 2591; G. Treboux, P. Lapstun, K. Silverbruck, *J. Phys. Chem.* **1999**, *103*, 1871.

[14] R. Saito, G. Dresselhaus, M. S. Dresselhaus, *Physical Properties of Carbon Nanotubes*, World Scientific, Singapur, **1998**; T. W. Ebbesen, H. J. Lezec, H. Hiura, J. W. Bennett, H. F. Ghaemi, T. Thio, *Nature* **1996**, *382*, 54.

[15] M. M. J. Treacy, T. W. Ebbeson, J. M. Gibson, *Nature* **1996**, *381*, 678.

[16] W. Han, Y. Bando, K. Kurahima, T. Sato, *Appl. Phys. Lett.* **1998**, *73*, 3085; D. Goldberg, W. Han, Y. Bando, L. Bourgeois, K. Kurahima, T. Sato, *J. Appl. Phys.* **1999**, *86*, 2364; E. Bengu, L. D. Marks, *Phys. Rev. Lett.* **2001**, *86*, 2385.

[17] B. C. Satishkumar, A. Govindaraj, K. R. Harikumar, J.-P. Zhang, A. K. Cheetham, C. N. R. Rao, *Chem. Phys. Lett.* **1999**, *300*, 473.

[18] W. Tremel, *Angew. Chem.* **1999**, *111*, 2311; *Angew. Chem. Int. Ed.* **1999**, *38*, 2175; R. Tenne, A. K. Zettl, *Top. Appl. Phys.* **2001**, *80*, 81; R. Nesper, G. Patzke, *Nachr. Chem. Tech. Lab.* **2001**, *49*, 886; R. Tenne, *Prog. Inorg. Chem.* **2001**, *50*, 269.

[19] Y. Rosenfeld Hacohen, E. Grunbaum, R. Tenne, J. Sloan, J. L. Hutchison, *Nature* **1998**, *395*, 336.

[20] Y. Li, J. Wang, Z. Deng, Y. Wu, X. Sun, D. Yu, P. Yang, *J. Am. Chem. Soc.* **2001**, *123*, 9904.

[21] C. J. Brumlik, C. R. Martin, *J. Am. Chem. Soc.* **1991**, *113*, 3174; C. R. Martin, M. Nishizawa, K. Jirage, M. Kang, *J. Phys. Chem. B* **2001**, *105*, 1925; S. B. Lee, C. R. Martin, *Chem. Mater.* **2001**, *13*, 3236.

[22] J. Bao, C. Tie, Z. Xu, Q. Zhou, D. Shen, Q. Ma, *Adv. Mater.* **2001**, *13*, 1631.

[23] B. Mayers, Y. Xia, *Adv. Mater.* **2002**, *14*, 279.

[24] The transmission electron microscopy (TEM) images shown in this paper were recorded on a CM30 microscope (Philips, Eindhoven, acceleration voltage 300 kV, point resolution 0.2 nm). Scanning electron microscopy (SEM) was performed on a LEO 1530 Gemini, which was operated at low voltage (usually 1 kV) to avoid charging of the uncoated, as-synthesized samples. The SEM image in Figure 7b was taken with an Hitachi S-900 microscope (courtesy of Dr. Martin Müller, ETH Zürich).

[25] G. Heurung, R. Gruehn, *Z. Anorg. Allg. Chem.* **1982**, *491*, 101.

[26] W. B. Hu, Y. Q. Zhu, W. K. Hsu, B. H. Chang, M. Terrones, N. Grobert, H. Terrones, J. P. Hare, H. W. Kroto, D. R. M. Walton, *Appl. Phys. A* **2000**, *70*, 231.

[27] L. Vayssieres, K. Keis, A. Hagfeldt, S.-E. Lundquist, *Chem. Mater.* **2001**, *13*, 4395.
[28] G. A. Kakos, T. W. Turney, T. B. Williams, *J. Solid State Chem.* **1994**, *108*, 102.
[29] R. Lauterbach, W. Schnick, *J. Mater. Sci.* **2000**, *35*, 3793.
[30] J. Hu, B. Deng, Q. Lu, K. Tang, R. Jiang, Y. Qian, G. Zhou, H. Cheng, *Chem. Commun*. **2000**, 715.
[31] E. Makovicky, B. G. Hyde, *Struct. Bonding (Berlin, Ger.)* **1981**, *46*, 101.
[32] P. Millet, J. Y. Henry, F. Mila, J. Galy, *J. Solid State Chem.* **1999**, *147*, 676.
[33] M. Remskar, A. Mrzel, Z. Skraba, A. Jesih, M. Ceh, J. Demšar, P. Stadelmann, F. Levy, D. Mihailovic, *Science* **2001**, *292*, 479.
[34] P. M. Ajayan, O. Stephan, P. Redlich, C. Colliex, *Nature* **1995**, *375*, 564.
[35] R. Nesper, M. E. Spahr, M. Niederberger, P. Bitterli, Int. Patent Appl. PCT/CH97/00470, **1997**; M. E. Spahr, P. Bitterli, R. Nesper, M. Müller, F. Krumeich, H.-U. Nissen, *Angew. Chem.* **1998**, *110*, 1339; *Angew. Chem. Int. Ed.* **1998**, *37*, 1263; F. Krumeich, H.-J. Muhr, M. Niederberger, F. Bieri, B. Schnyder, R. Nesper, *J. Am. Chem. Soc.* **1999**, *121*, 8324; H.-J. Muhr, F. Krumeich, U. P. Schönholzer, F. Bieri, M. Niederberger, L. J. Gauckler, R. Nesper, *Adv. Mater*. **2000**, *12*, 231.
[36] R. Nesper, H.-J. Muhr, M. Niederberger, Int. Patent Appl. PCT/CH00/00570, **2000**; M. Niederberger, H.-J. Muhr, F. Krumeich, F. Bieri, D. Günther, R. Nesper, *Chem. Mater*. **2000**, *12*, 1995.
[37] M. Niederberger, Dissertation No. 13971, ETH, Zürich, **2000**.
[38] F. Bieri, F. Krumeich, H.-J. Muhr, R. Nesper, *Helv. Chim. Acta* **2001**, *84*, 3015.
[39] F. Krumeich, H.-J. Muhr, M. Niederberger, F. Bieri, R. Nesper, *Z. Anorg. Allg. Chem.* **2000**, *626*, 2208.
[40] X. Wang, L. Liu, R. Bontchev, A. J. Jacobson, *Chem. Commun.* **1998**, 1009.
[41] M. Wörle, J. de Onate, H.-J. Muhr, F. Bieri, R. Nesper, *Chimia* **1999**, *53*, 336; M. Wörle, F. Krumeich, H.-J. Muhr, F. Bieri, R. Nesper, unpublished results.
[42] F. Krumeich, H.-J. Muhr, M. Niederberger, F. Bieri, M. Reinoso, R. Nesper, *Mater. Res. Soc. Symp. Proc.* **2000**, *581*, 393.
[43] J. M. Reinoso, H.-J. Muhr, F. Krumeich, F. Bieri, R. Nesper, *Helv. Chim. Acta* **2000**, *83*, 1724.
[44] M. E. Spahr, P. Stoschitzki-Bitterli, R. Nesper, O. Haas, P. Novák, *J. Electrochem. Soc.* **1999**, *146*, 2780; S. Nordlinder, K. Edström, T. Gustafsson, *Electrochem. Solid-State Lett.* **2001**, *4*, A129; A. Dobley, K. Ngala, S. Yang, P. Y. Zavalij, M. S. Whittingham, *Chem. Mater.* **2001**, *13*, 4382.
[45] M. E. Spahr, Dissertation Nr. 12281, ETH, Zürich, **1997**.
[46] K. S. Pillai, F. Krumeich, H.-J. Muhr, M. Niederberger, R. Nesper, *Solid State Ionics* **2001**, *141–142*, 185.
[47] P. Hoyer, *Langmuir* **1996**, *12*, 1411.
[48] H. Imai, Y. Takei, K. Shimizu, M. Matsuda, H. Hirahima, *J. Mater. Chem.* **1999**, *9*, 2971; M. Zhang, Y. Bando, K. Wada, *J. Mater. Sci. Lett.* **2001**, *20*, 167; S. M. Liu, L. M. Gan, L. H. Liu, W. D. Zhang, H. C. Zeng, *Chem. Mater*. **2002**, *14*, 1391.
[49] S. Kobayashi, K. Hanabusa, N. Hamasaki, M. Kimura, H. Shirai, *Chem. Mater*. **2000**, *12*, 1523.
[50] R. A. Caruso, J. H. Schattka, A. Greiner, *Adv. Mater*. **2001**, *13*, 1577.
[51] D. Gong, C. A. Grimes, O. K. Varghese, W. Hu, R. S. Singh, Z. Chen, E. C. Dickey, *J. Mater. Res.* **2001**, *16*, 3331.
[52] T. Kasuga, M. Hiramutsu, A. Hoson, T. Sekino, K. Niihara, *Langmuir* **1998**, *14*, 3160; T. Kasuga, M. Hiramutsu, A. Hoson, T. Sekino, K. Niihara, *Adv. Mater*. **1999**, *11*, 1307.
[53] G. H. Du, Q. Chen, R. C. Che, Z. Y. Yuan, L. M. Peng, *Appl. Phys. Lett.* **2001**, *79*, 3702.
[54] K. S. Pillai, F. Krumeich, R. Nesper, unpublished results.
[55] E. Müller, F. Krumeich, *Ultramicroscopy* **2000**, *84*, 143.
[56] F. Liebau, *Structural Chemistry of Silicates*, Springer, Berlin, **1995**.
[57] K. Yada, *Acta Crystallogr. Sect. A* **1971**, *27*, 659.
[58] H.-P. Lin, C.-Y. Mou, S.-B. Liu, *Adv. Mater*. **2000**, *12*, 103.
[59] C. T. Kresge, M. E. Leonowicz, W. J. Roth, J. C. Vartuli, J. S. Beck, *Nature* **1992**, *359*, 710.
[60] Z. L. Wang, R. P. Gao, J. L. Gole, J. D. Stout, *Adv. Mater*. **2000**, *12*, 1938.
[61] J. H. Jung, Y. Ono, S. Shinkai, *Langmuir* **2000**, *16*, 1643.
[62] C. Hippe, M. Wark, E. Lork, G. Schulz-Ekloff, *Microporous Mesoporous Mater.* **1999**, *31*, 235.
[63] R. A. Caruso, M. Antonietti, *Chem. Mater.* **2001**, *13*, 3272.
[64] B. C. Satishkumar, A. Govindaraj, E. M. Vogl, L. Baumallick, C. N. R. Rao, *J. Mater. Res.* **1997**, *12*, 604.
[65] B. C. Satishkumar, A. Govindaraj, M. Nath, C. N. R. Rao, *J. Mater. Chem.* **2000**, *10*, 2115.
[66] C. N. R. Rao, B. C. Satishkumar, A. Govindaraj, *Chem. Commun.* **1997**, 1581.
[67] J. S. Beck, J. C. Vartuli, W. J. Roth, M. E. Leonowicz, C. T. Kresge, K. D. Schmidt, C. T. W. Chu, D. H. Olson, E. W. Sheppard, S. B. McCullen, J. B. Higgins, J. C. Schlenker, *J. Am. Chem. Soc.* **1992**, *114*, 10834.
[68] L. Pu, X. Bao, J. Zou, D. Feng, *Angew. Chem.* **2001**, *113*, 1538; *Angew. Chem. Int. Ed.* **2001**, *40*, 1490.
[69] J. C. Hulteen, C. R. Martin, *J. Mater. Chem.* **1997**, *7*, 1075.
[70] B. Cheng, E. T. Samulski, *J. Mater. Chem.* **2001**, *11*, 2901.
[71] B. A. Hernandez, K.-S. Chang, E. R. Fisher, P. K. Dorhout, *Chem. Mater.* **2002**, *14*, 480.
[72] B. B. Lakshmi, P. K. Dorhout, C. R. Martin, *Chem. Mater.* **1997**, *9*, 857.
[73] A. Birner, R. B. Wehrspohn, U. M. Gösele, K. Busch, *Adv. Mater.* **2001**, *13*, 377.
[74] L.-C. Qin, X. Zhao, K. Hirahara, Y. Miyamoto, Y. Ando, S. Iijima, *Nature* **2000**, *408*, 50.
[75] L. Dai, A. W. H. Mau, *Adv. Mater.* **2001**, *13*, 899; G. Gu, G. Philipp, X. Wu, M. Burghard, A. M. Bittner, S. Roth, *Adv. Funct. Mater.* **2001**, *11*, 295.
[76] L. C. Otero-Díaz, R. Withers, A. Gómez-Herrero, T. R. Welberry, S. Schmid, *J. Solid State Chem.* **1995**, *115*, 274; A. Gómez-Herrero, A. R. Landa-Cánovas, S. Hansen, L. C. Otero-Díaz, *Micron* **2000**, *31*, 587.
[77] D. Bernaerts, S. Amelinckx, G. Van Tendeloo, J. Van Landuyt, *J. Cryst. Growth* **1997**, *172*, 433; D. Bernaerts, S. Amelinckx, G. Van Tendeloo, J. Van Landuyt, *J. Phys. Chem. Solids* **1997**, *58*, 1807.
[78] R. Tenne, L. Margulis, M. Genut, G. Hodes, *Nature* **1992**, *360*, 444.
[79] R. Tenne, M. Homyonfer, Y. Feldman, *Chem. Mater.* **1998**, *10*, 3225; A. Rothschild, G. L. Frey, M. Homyonfer, R. Tenne, M. Rappaport, *Mater. Res. Innovations* **1999**, *3*, 145; A. Rothschild, J. Sloan, R. Tenne, *J. Am. Chem. Soc.* **2000**, *122*, 5169; A. Rothschild, R. Popovitz-Biro, O. Lourie, R. Tenne, *J. Phys. Chem. B* **2000**, *104*, 8976; Y. Q. Zhu, W. K. Hsu, N. Grobert, B. H. Chang, M. Terrones, H. Terrones, H. W. Kroto, D. R. M. Walton, *Chem. Mater.* **2000**, *12*, 1190.
[80] M. Remškar, Z. Škraba, M. Regula, C. Ballif, R. Sanjinés, F. Lévy, *Adv. Mater.* **1998**, *10*, 246.
[81] Y. D. Li, X. L. Li, R. R. He, J. Zhu, Z. X. Deng, *J. Am. Chem. Soc.* **2002**, *124*, 1411.
[82] A. Rothschild, S. R. Cohen, R. Tenne, *Appl. Phys. Lett.* **1999**, *75*, 5169.
[83] Y. Feldman, E. Wasserman, D. J. Srolovitz, R. Tenne, *Science* **1995**, 267, 222.
[84] M. Remškar, Z. Škraba, F. Cléton, R. Sanjinés, F. Lévy, *Appl. Phys. Lett.* **1996**, *69*, 351; M. Zelinski, P. K. Dorhout, *J. Am. Chem. Soc.* **1998**, *120*, 734; W. K. Hsu, B. H. Chang, Y. Q. Zhu, W. Q. Han, H. Terrones, M. Terrones, N. Grobert, A. K. Cheetham, H. W. Kroto, D. R. M. Walton, *J. Am. Chem. Soc.* **2000**, *122*, 10155; M. Nath, A. Govindaraj, C. N. R. Rao, *Adv. Mater.* **2001**, *13*, 283.
[85] Y. Q. Zhu, W. K. Hsu, M. Terrones, S. Firth, N. Grobert, R. J. H. Clark, H. W. Kroto, D. R. M. Walton, *Chem. Commun.* **2001**, 121.
[86] M. Nath, C. N. R. Rao, *J. Am. Chem. Soc.* **2001**, *123*, 4841.
[87] M. Nath, C. N. R. Rao, *Chem. Commun.* **2001**, 2236.
[88] R. L. D. Whitby, W. K. Hsu, C. B. Boothroyd, P. K. Fearon, H. W. Kroto, D. R. M. Walton, *ChemPhysChem* **2001**, *2*, 620.
[89] Y. Q. Zhu, W. K. Hsu, H. W. Kroto, D. R. M. Walton, *Chem. Commun.* **2001**, 2184.
[90] G. Seifert, H. Terrones, M. Terrones, T. Frauenheim, *Solid State Commun.* **2000**, *115*, 635.
[91] G. Seifert, H. Terrones, M. Terrones, G. Jungickel, T. Frauenheim, *Solid State Commun.* **2000**, *114*, 245; G. Seifert, T. Köhler, R. Tenne, *J. Phys. Chem. B* **2002**, *106*, 2497.

[92] L. Rapoport, Y. Feldman, M. Homyonfer, H. Cohen, J. Sloan, J. L. Hutchison, R. Tenne, *Wear* **1999**, *229*, 975; M. Chhowalla, G. A. J. Amaratunga, *Nature* **2000**, *407*, 164; C. Drummond, N. Alcantar, J. Israelachvili, R. Tenne, Y. Golan, *Adv. Funct. Mater.* **2001**, *11*, 348.

[93] J. Chen, N. Kuriyama, H. Yuan, H. T. Takeshita, T. Sakai, *J. Am. Chem. Soc.* **2001**, *123*, 11813.

[94] J. A. Hollingsworth, D. M. Poojary, A. Clearfield, W. E. Buhro, *J. Am. Chem. Soc.* **2000**, *122*, 3562.

[95] C. N. R. Rao, A. Govindaraj, F. L. Deepak, N. A. Gunari, M. Nath, *Appl. Phys. Lett.* **2001**, *78*, 1853.

[96] M. Cote, M. L. Cohen, D. J. Chadi, *Phys. Rev. B* **1998**, *58*, R4277.

[97] E. Leontidis, T. Kyprianidou-Leodidou, F. Krumeich, W. Caseri, unpublished results.

[98] S. M. Lee, Y. H. Lee, Y. G. Hwang, J. Elsener, D. Porezag, T. Frauenheim, *Phys. Rev. B* **1999**, *60*, 7788.

[99] G. Seifert, T. Frauenheim, *J. Korean Phys. Soc.* **2000**, *37*, 89.

[100] G. Seifert, T. Köhler, K. U. Urbassek, E. Hernàndez, T. Frauenheim, *Phys. Rev. B* **2001**, *63*, 193409.

[101] G. Seifert, T. Köhler, Z. Hajnal, T. Frauenheim, *Solid State Commun.* **2001**, *119*, 653.

[102] D. Wichmann, K. Jug, *J. Phys. Chem. B* **1999**, *103*, 10087.

[103] M. Brändle, R. Nesper, unpublished results. Lattice energy minimizations of the V_2O_5 double layer tubes (space group *P4mmm*) and the planar V_2O_5 double layer (space group *Pmmm*) employed a DFT-parametrized shell model potential for vanadium oxides. The tubes and the double layers were arranged in periodic orthorhombic boxes. Both were allowed to relax freely within their space group constraints and under constant pressure conditions along the tube axis and the layer plane directions. Shell model parameters were obtained from fitting to the energy gradients of optimized and distorted vanadium oxide clusters that were saturated with OH groups. The saturation was chosen so that the total electron count of the cluster and the formal charge of the vanadium ions (+5) were correct. Cluster energies and gradients were obtained from DFT/B3LYP calculations with a DZP basis set for H and V and a TZP basis set for O (A. Schäfer, H. Horn, R. Ahlrichs, *J. Chem. Phys.* **1992**, *97*, 2571). TURBOMOLE (R. Ahlrichs, M. Bär, M. Häser, H. Horn, C. Kölmel, *Chem. Phys. Lett.* **1995**, *162*, 165; O. Treutler, R. Ahlrichs, *J. Chem. Phys.* **1995**, *102*, 346) was used for the DFT calculations. GULP was used for the fitting and for all periodic calculations (J. D. Gale, *J. Chem. Soc., Faraday Trans.* **1997**, *93*, 629). The clusters $[VO(OH)_3]$ (C_{3v}) and $[VO(OH)_3]_2$ (C_{3v}) (both clusters with trigonal tetracoordination of V) and $V_6O_{21}H_{12}$ (C_{2v}), $V_6O_{20}H_{10}$ (C_{2v}), $[V_6O_{20}H_{10}]_2$ (C_{3v}), $V_3O_7H_{11}$ (C_s) and $[V_3O_7H_{11}]_2$ (C_s) (all clusters with pyramidal pentacoordination of V).

[104] S. Liu, J. Yue, A. Gedanken, *Adv. Mater.* **2001**, *13*, 656.

[105] N. R. Jana, L. Gearheart, C. J. Murphy, *Chem. Commun.* **2001**, 617.

[106] A. Abdelouas, W. L. Gong, W. Lutze, J. A. Shelnutt, R. Franco, I. Moura, *Chem. Mater.* **2000**, *12*, 1510.

[107] P. Chen, X. Wu, J. Lin, K. L. Tan, *J. Phys. Chem.* **1999**, *22*, 4559; Z. I. Zhang, B. Li, Z. J. Shi, Z. N. Gu, Z. Q. Xue, L.-M. Peng, *J. Mater. Res.* **2000**, *15*, 2658.

[108] B. Nikoobakht, Z. L. Wang, M. A. El-Sayed, *J. Phys. Chem. B* **2000**, *104*, 8635; B. R. Martin, D. J. Dermody, B. D. Reiss, M. Fang, L. A. Lyon, M. J. Natan, T. E. Mallouk, *Adv. Mater.* **1999**, *11*, 1021.

[109] Y. Wu, H. Yan, M. Huang, B. Messer, J. H. Song, P. Yang, *Chem. Eur. J.* **2002**, *8*, 1260.

[110] X. Duan, C. M. Lieber, *Adv. Mater.* **2000**, *12*, 298.

[111] L. Manna, E. C. Scher, A. P. Alivisatos, *J. Am. Chem. Soc.* **2000**, *122*, 12700.

[112] Z. W. Pan, H.-L. Lai, F. C. K. Au, X. Duan, W. Zhou, W. Shi, N. Wang, C.-S. Lee, N.-B. Wong, S.-T. Lee, S. Xie, *Adv. Mater.* **2000**, *12*, 1186.

[113] K. Tang, Y. Qian, *Appl. Phys. Lett.* **1999**, *75*, 507.

[114] P. D. Yang, C. M. Lieber, *Science* **1996**, *273*, 1836.

[115] A recent paper reports the synthesis of various oxide nanorods by a combination of a sol–gel reaction and electrophoretic deposition. S. J. Limmer, S. Seraji, T. P. Chou, C. Nguyen, G. Cao, *Adv. Funct. Mater.* **2002**, *12*, 59.

[116] K. Byrappa, M. Yoshimura, *Handbook of Hydrothermal Technology*, Noyes, Park Ridge, N.J., **2001**.

[117] G. R. Patzke, F. Krumeich, R. Nesper, unpublished results.

[118] I. Böschen, B. Krebs, *Acta Crystallogr. Sect. B* **1974**, *30*, 1795.

[119] J. R. Günter, *J. Solid State Chem.* **1972**, *5*, 354.

[120] W. Zhang, S. T. Oyama, *J. Phys. Chem.* **1996**, *100*, 10759.

[121] R. Martell, H. R. Shea, P. Avouris, *Nature* **1999**, *398*, 299.

[122] M. Li, H. Schnablegger, S. Mann, *Nature* **1999**, *402*, 393.

[123] L. Qi, H. Cölfen, M. Antonietti, M. Li, J. D. Hopwood, A. J. Ashley, S. Mann, *Chem. Eur. J.* **2001**, *7*, 3526.

[124] S. Kwan, F. Kim, J. Akana, P. Yang, *Chem. Commun.* **2001**, 447.

[125] Z. W. Pan, Z. R. Dai, Z. L. Wang, *Science* **2001**, *291*, 1947.

[126] H.-W. Liao, Y.-F. Wang, X.-M. Liu, Y.-D. Li, Y.-T. Qian, *Chem. Mater.* **2000**, *12*, 2819.

[127] B. B. Lakshmi, C. J. Patrissi, C. R. Martin, *Chem. Mater.* **1997**, *9*, 2544.

[128] W. Wang, Y. Zhan, G. Wang, *Chem. Commun.* **2001**, 727.

[129] N. Beermann, L. Vayssieres, S.-E. Lindquist, A. Hagfeldt, *J. Electrochem. Soc.* **2000**, *147*, 2456.

[130] R. Kumar, Y. Koltypin, X. N. Xu, Y. Yeshurun, A. Gedanken, I. Felner, *J. Appl. Phys.* **2001**, *89*, 6324.

[131] Y. C. Choi, W. S. Kim, Y. S. Park, S. M. Lee, D. J. Bae, Y. H. Lee, G.-S. Park, W. B. Choi, N. S. Lee, G. M. Kim, *Adv. Mater.* **2000**, *12*, 746.

[132] J. Y. Li, Z. Y. Qiao, X. L. Chen, L. Chen, Y. G. Cao, M. He, H. Li, Z. M. Cao, Z. Zhang, *J. Alloys Compd.* **2000**, *306*, 300.

[133] H. Z. Zhang, Y. C. Kong, Y. Z. Wang, X. Du, Z. G. Bai, J. J. Wang, D. P. Yu, Y. Ding, Q. L. Hang, S. Q. Feng, *Solid State Commun.* **1999**, *109*, 677.

[134] W. Q. Han, P. Kohler-Redlich, F. Ernst, M. Rühle, *Solid State Commun.* **2000**, *115*, 527.

[135] G.-S. Park, W.-B. Choi, J.-M. Kim, Y. C. Choi, Y. H. Lee, C.-B. Lim, *J. Crystal Growth* **2000**, *220*, 494.

[136] C. C. Tang, S. S. Fan, M. L. de la Chapelle, P. Li, *Chem. Phys. Lett.* **2001**, *333*, 12.

[137] Y. Zhang, J. Zhu, Q. Zhang, Y. Yan, N. Wang, X. Zhang, *Chem. Phys. Lett.* **2000**, *317*, 504.

[138] C. Liang, G. Meng, Y. Lei, F. Phillipp, L. Zhang, *Adv. Mater.* **2001**, *13*, 1330.

[139] G. L. Li, M. Liu, G. H. Wang, *J. Mater. Res.* **2001**, *16*, 3614.

[140] Z. Cui, G. W. Meng, W. D. Huang, G. Z. Wang, L. D. Zhang, *Mater. Res. Bull.* **2000**, *35*, 1653.

[141] Y. Li, M. Sui, Y. Ding, G. Zhang, J. Zhuang, C. Wang, *Adv. Mater.* **2000**, *12*, 818.

[142] X. Wang, Y. Li, *J. Am. Chem. Soc.* **2002**, *124*, 2880.

[143] R. Nesper, F. Krumeich, M. Niederberger, A. Baiker, F. Eigenmann, Eur. Patent Appl. 01810072.7, **2001**; M. Niederberger, F. Krumeich, H.-J. Muhr, M. Müller, R. Nesper, *J. Mater. Chem.* **2001**, *11*, 1941.

[144] S. J. Limmer, S. Seraji, M. J. Forbess, Y. Wu, T. P. Chou, C. Nguyen, G. Cao, *Adv. Mater.* **2001**, *13*, 1269.

[145] L. Guo, Z. Wu, T. Liu, W. Wang, H. Zhu, *Chem. Phys. Lett.* **2000**, *318*, 49.

[146] Y. Liu, C. Zheng, W. Wang, Y. Zhan, G. Wang, *J. Crystal Growth* **2001**, *233*, 8.

[147] W.-J. Kim, S.-M. Yang, *Adv. Mater.* **2001**, *13*, 1191.

[148] M. Zhang, Y. Bando, K. Wada, *J. Mater. Sci. Lett.* **2001**, *20*, 167.

[149] J. Livage, *Chem. Mater.* **1991**, *3*, 578.

[150] Y. F. Zhang, Y. H. Tang, X. F. Duan, Y. Zhang, C. S. Lee, N. Wang, I. Bello, S. T. Lee, *Chem. Phys. Lett.* **2000**, *323*, 180.

[151] J. Y. Li, X. L. Chen, H. Li, M. He, Z. Y. Qiao, *J. Crystal Growth* **2001**, *233*, 5.

[152] M. H. Huang, S. Mao, H. Feick, H. Yan, Y. Wu, H. Kind, E. Weber, R. Russo, P. Yang, *Science* **2001**, *292*, 1897.

[153] C. Pacholski, A. Kornowski, H. Weller, *Angew. Chem.* **2002**, *114*, 1234; *Angew. Chem. Int. Ed.* **2002**, *41*, 1188.